Nanoscale

Accepted Manuscript

This article can be cited before page numbers have been issued, to do this please use: H. Tohati, A. Pekker, P. Andrievi, L. Forro, B. Náfrádi , M. Kollár, E. Horvath and K. Kamaras, *Nanoscale*, 2017, DOI: 10.1039/C7NR06136F.

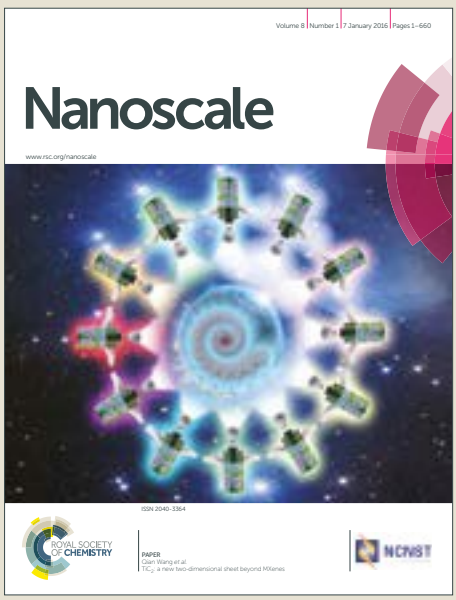

ROYAL SOCIETY OF CHEMISTRY

rsc.li/nanoscale

View Article Online
DOI: 10.1039/C7NR06136F

Journal Name

ARTICLE TYPE

Cite this: DOI: 10.1039/xxxxxxxxxx

Optical detection of charge dynamics in $CH_3NH_3PbI_3$/carbon nanotube composites†

Hajnalka M. Tóháti,[a] Áron Pekker,*[a] Pavao Andričević,[b] László Forró,[b] Bálint Náfrádi,[b] Márton Kollár, [b] Endre Horváth,[b] and Katalin Kamarás[a]

Received Date
Accepted Date

DOI: 10.1039/xxxxxxxxxx

www.rsc.org/journalname

We have investigated the optical absorption of metallic and semiconducting carbon nanotubes/$CH_3NH_3PbI_3$ micro- and nanowire composites. Upon visible light illumination semiconducting carbon nanotube based samples show a photo-induced doping, originating from the charge carriers created in the perovskite while this kind of change is absent in the composites containing metallic nanotubes, due to their strikingly different electronic structure. The response in the nanotubes shows, beside a fast diffusion of photo-generated charges, a slow component similar to that observed in pristine $CH_3NH_3PbI_3$ attributed to structural rearrangement, and leading to slight, light induced changes of the optical gap of the perovskite. This charge transfer from the illuminated perovskite confirms that carbon nanotubes (especially semiconducting ones) can form efficient charge-transporting layers in the novel organometallic perovskite based optoelectronic devices.

1 Introduction

Third generation photovoltaic devices have recently generated great interest because of their low cost and high efficiency potential. Organic-inorganic metal halide perovskites, especially methylammonium lead iodide ($CH_3NH_3PbI_3$, henceforth referred to as $MAPbI_3$) emerged as front runners in this generation due to their excellent optoelectronic properties such as high absorption coefficient, high mobility, long and balanced carrier diffusion and low exciton binding energy.[1–5] These perovskite solar cells have achieved efficiencies above 20%[6,7] within a period shorter than any other material proposed for solar energy conversion. They are approaching the efficiency of commercial c-Si solar cells. However, there are still shortcomings that prevent these cells from getting to the market, one being the high cost and stability issues of the hole-selective transport layer (HTM) in the cell. The most common HTM material, with which the highest power conversion efficiencies have been obtained, is 2,2',7,7'-tetrakis(N,N-di-p-methoxyphenyl-amine)9,9'-spirobifluorene (Spiro-OMeTAD).[8]

Recently, carbon nano-materials, such as nanoparticles, carbon nanotubes (CNTs) and graphene flakes are being reported as good alternatives for HTM materials.[9–13] Especially, CNTs are very attractive candidates, since they have been already used successfully in various optoelectronic applications, like light-emitting diodes, photodetectors, phototransistors[14,15] and other photovoltaic cells, due to their direct band gap (when they are semiconducting) and outstanding electronic and mechanical properties.[16] Not only did they show comparable performance to conventional architectures, but they also provided devices with improved features such as stability, reduction of the hysteretic and drift effects,[17,18] flexibility[19] and semi-transparency.[20] Therefore, to be able to increase further the performance of perovskite-CNT based devices it is important to learn more about the interface between the perovskites and the different types of CNTs. Especially, it is essential to understand the details of the charge transfer from the illuminated photovoltaic perovskite to the CNTs.

Several studies of the subject have already been published,[9,21,22] strongly suggesting photoinduced charge transfer between CNTs and perovskites that leads to mobile charge carriers in the system. These studies were mainly based on the bleaching of the first excitonic optical transition (S_{11}) of semiconducting nanotubes. The presence of mobile carriers was concluded from photocurrent measurements[9] and from time-resolved microwave conductivity at 9 GHz[22]. Charge transfer between the CNTs and the perovskite layer was further inferred from photoemission spectroscopy[21] and the dynamics of the process was determined on a time scale less than a millisecond. All these measurements were conducted in device architectures, thus reflecting the processes of all layers and interfaces.

In this work we use a simple $MAPbI_3$/CNT hybrid system in or-

[a] Institute for Solid State Physics and Optics, Wigner Research Centre for Physics, Hungarian Academy of Sciences, 1525 Budapest, Hungary. E-mail: pekker.aron@wigner.mta.hu
[b] Laboratory of Physics of Complex Matter (LPMC), Ecole Polytechnique Fédérale de Lausanne, 1015 Lausanne, Switzerland.

† Electronic Supplementary Information (ESI) available. See DOI: 10.1039/b000000x/

View Article Online
DOI: 10.1039/C7NR06136F

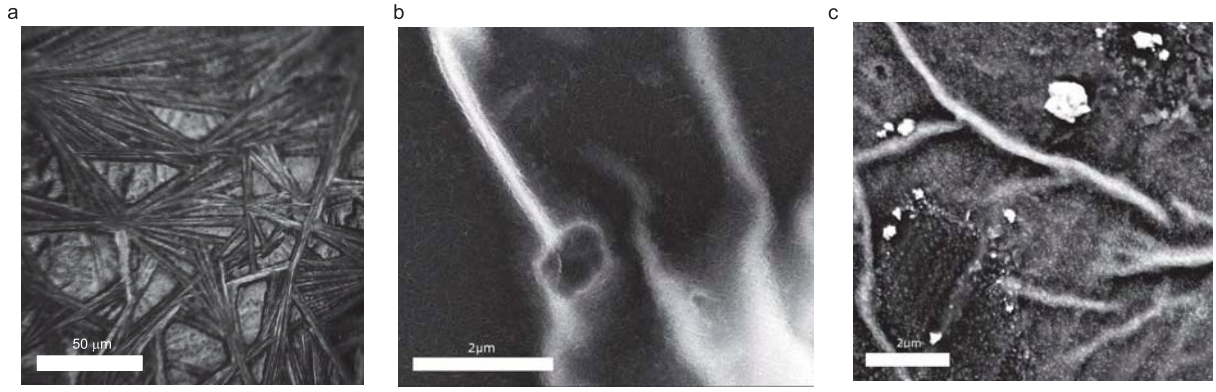

Fig. 1 a) Optical image of a (mixed s-m) CNT/$MAPbI_3$ composite prepared for measurement (the scale bar is 50μm). First, elongated micro- and nanocrystallites of $MAPbI_3$/DMF solvatomorph precursor phase were grown. The $MAPbI_3$ wires were formed by subsequent solvent evaporation, while preserving the elongated crystal shape. These wires are sitting on a 100 nm thick dense mat of self-supporting carbon nanotubes. b) SEM image of $MAPbI_3$/DMF drop casted on a CNT film measured by back scattered electron detector (resolution good for CNT, limited for $MAPbI_3$, the scale bar is 2μm). c) SEM image of $MAPbI_3$/DMF drop casted on a CNT film measured by secondary electron detector (resolution limited for CNT, good for $MAPbI_3$, the scale bar is 2μm).

der to restrict our observations to the one interface between these constituents, and extend the study of charge transport to longer wavelengths and longer time scales. We report the charge transfer between $MAPbI_3$ and CNTs upon white light illumination by using mid-infrared (MIR) and near-infrared (NIR) optical spectroscopy. In the MIR range, we follow the appearance upon illumination of free-carrier (Drude) absorption, correlated with the photobleaching of the S_{11} transition in the NIR, thus establishing the charge migration through the interface as the source of photocurrent under operating conditions of solar cells. The dynamics of the process extends to the timescale of tens of minutes, connecting the charge migration to structural changes in the perovskite.[23–25] A comparison between two high purity nanotube samples is given in order to illustrate the difference between semiconducting and metallic nanotube enriched samples. We find that semiconducting nanotubes show a distinct advantage over metallic ones regarding photoinduced charge transport, confirming the choice of previous studies to apply semiconducting[21,22] or functionalized[9] carbon nanotubes in similar architectures. Furthermore, we prove that there is no severe chemical reaction establishing covalent bonds between the nanotubes and the perovskite during the synthesis of the composite system. The processes studied here can form the basis of further possible optolectronic applications of the $MAPbI_3$-semiconducting nanotube ensemble beyond solar cells, mentioned above.

2 Experimental methods

High purity commercially available single-walled carbon nanotube samples (NanoIntegris Inc.) were used for this study, prepared from arc-derived carbon nanotubes (mean diameter 1.4 nm) by density gradient ultracentrifugation.[26] Two different types of samples were investigated: one batch was enriched with 95% semiconducting (s-CNTs) and another with 95% metallic (m-CNTs) nanotube content. Spectroscopic studies were carried out on self-supporting nanotube thin films. Preparation of the nanotube samples was done by vacuum filtration and wet transfer.[27] The thin films were annealed at 200 °C in vacuum for 10 hours to remove moisture and solvent residues. $MAPbI_3$ single crystals were prepared according to Poglitsch and Weber.[28] The harvested single crystals were dissolved in N,N-dimethylformamide. The concentration of the solution was 114 mg/ml. The composite CNT/$MAPbI_3$ samples were prepared by drop casting 4 μl solution of $MAPbI_3$ in N,N-dimethylformamide (DMF) on self-supporting CNT films, resulting in micrometer-sized wires described earlier.[15,29] The composite samples were dried in air for 30 min at 80 °C.

The possible chemical reaction at the CNT/$MAPbI_3$ interface was excluded by Raman measurements, since the D and G bands did not change with respect to the pristine CNTs (Supporting Information, Fig. S1). The samples were characterized by mid-infrared (MIR) and near-infrared (NIR) spectroscopy. The MIR and NIR measurements were performed in a dry nitrogen purged Bruker Tensor 27 FTIR spectrometer. For the illumination a 3 W white light emitting diode (LED) was used. In order to cut off the high energy part of the LED light, a 500 nm long-pass filter was applied. The samples were kept in dark before the measurements and illuminated only with the LED light. SEM images were taken with a Quanta 3D (FEI) scanning electron microscope using a back scattered electron detector and an LVEM5 (Delong America Inc.) electron microscope using a secondary electron detector.

3 Results and Discussion

Typical images of the composite samples are summarized in Fig. 1. Figure 1a shows the optical image of the sample where the micrometer-wide wires of $MAPbI_3$ are supported by the CNT film. It is likely that such a texture of the perovskite is caused by the solvent and/or by the CNT substrate. Figure 1b shows a scanning electron microscope (SEM) image of a similar CNT/$MAPbI_3$ sample. This image was taken using a back scattered electron detector which enables good resolution on the pristine carbon nanotube network (dark gray regions) but fails to capture the details of the $MAPbI_3$ crystals (bright regions). To complement this limitation we have taken another image with similar magnification using a secondary electron detector showing the $MAPbI_3$ crystals formed on the nanotube mat (Fig. 1c). These nanocrystals are similar

View Article Online
DOI: 10.1039/C7NR06136F

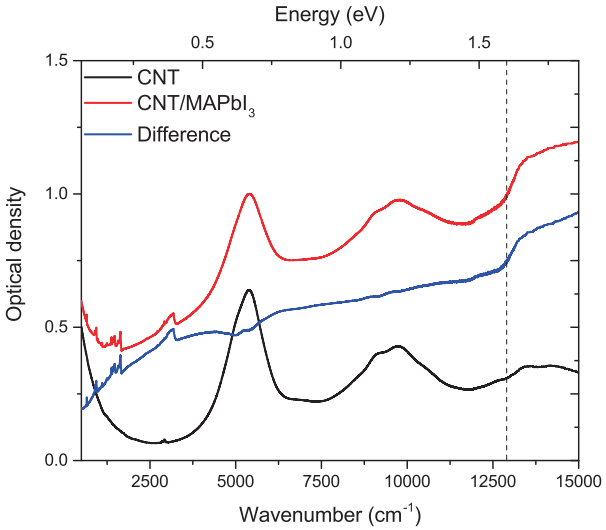

Fig. 2 Effect of $MAPbI_3$ on the CNT spectrum. Black - spectrum of pristine nanotube sample. Red - spectrum of the nanotube/$MAPbI_3$ composite sample. Blue - difference spectrum. The dashed line indicates the band gap of $MAPbI_3$.

in size (10 - 50 nm) to what has been found in perovskite/CNT hybrid materials reported by Ka et. al.[30]

To investigate the effect of visible light illumination on the nanotube-$MAPbI_3$ composite samples we performed spectroscopic measurements in the 500-15000 cm^{-1} wavenumber range (0.06-1.85 eV). First, we were looking for indications of electronic interactions at the CNT/$MAPbI_3$ interface. The results using mixed (s-m) CNTs are given in Figure 2 without LED illumination (called "in dark"). The spectrum of the pristine nanotubes was measured first, and then $MAPbI_3$ was drop cast and dried. Figure 2 shows the optical density (-log(T), where T is the optical transmittance) spectra of the nanotube samples with (composite sample) and without $MAPbI_3$ (pristine sample). Optical density is the total loss of light through the sample, not corrected for reflectance; in this spectral region, it can be considered analogous to absorbance. The difference spectrum (Fig. 2 - blue) contains the changes due to the introduction of $MAPbI_3$. The NIR part shows a jump in the optical density around 1.6 eV which is consistent with the band gap of $MAPbI_3$.[1,31] The sloping baseline, increasing towards higher wavenumbers, is caused by light scattering on the nanoparticles. The molecular vibrational features, especially those related to methylammonium ions[32] and to DMF, show small variations mostly during the drying stage of the composite (Supporting Information, Fig. S2).

In order to investigate the electronic interaction between the CNTs and $MAPbI_3$ micro- and nanowires via photoresponse, we have performed a series of dark and LED illuminated measurements in the MIR spectral region. Figure 3 shows the effect of illumination on the spectrum of the composite samples (for the NIR response see Supporting Information, Fig. S3). To emphasize the changes induced by light we calculated the normalized difference spectrum: $\Delta A_{ON} = (T_d - T_i)/T_d$, where T_d is the transmission spectrum in the dark and T_i is the spectrum measured with the light source on. To test the reversibility of the process, we measured the samples after turning the light off, in this case the normalized difference spectrum was calculated in the following way: $\Delta A_{OFF} = (T_i - T_d)/T_i$. These ΔA values represent absorbance changes in the sample.

As one can see in Figure 3a, in case of semiconducting samples the light induced changes take place in two regions of the spectrum: in the low wavenumber part (<2000 cm^{-1}) which is dominated by the response of the free electrons in the nanotubes, and around 5300 cm^{-1} which for this type of nanotube corresponds to the difference between the first Van Hove singularities (S_{11}) of the semiconducting nanotubes.[33] (The feature in the 3000 cm^{-1} region is coming from the DMF and we omit its discussion). The changes in the two regions show different signs. Turning the light on, the intensity in the free carrier region of the difference spectrum increases while the S_{11} region decreases. When the light is turned off, the changes are reversed, the free carrier part is decreasing and S_{11} is gaining intensity. Figure 3b shows the results of the same measurements on m-CNT/$MAPbI_3$ composite samples. Compared to the s-CNT based composites the changes are significantly smaller.

The kind of redistribution of spectral weight that is presented in Figure 3a is reminiscent of doping[9,22]. The two characteristic spectra of the m- and s-CNT/$MAPbI_3$ upon illumination are compared to the spectrum of a semiconducting pristine nanotube sample doped by atmospheric oxygen (see Figure 4a), known to be p-type.[34] This comparison supports the interpretation that there is charge transfer from the illuminated $MAPbI_3$ to CNTs. Ihly et al.[22] have proven the presence of the free carriers in a multilayer device configuration containing s-SWNTs and $MAPbI_3$ by time-resolved microwave conductivity experiments at 9 GHz. The present observation narrows this effect spatially to the CNT/$MAPbI_3$ interface and at the same time extends it in frequency so the Drude-type behavior is apparent. We compare the change in the transmission ($\Delta T_{ON} = T_d - T_i$ and $\Delta T_{OFF} = T_i - T_d$) in Figure 4b. Since metallic nanotubes possess a higher Drude contibution by nature than the semiconducting ones, this comparison is more accurate in comparing changes of the different types of composites. It is clear from Figure 4b that the metallic composite sample shows negligible change in the low frequency region compared to the semiconducting sample. This indicates the absence of charge transfer upon illumination between the metallic nanotubes and the perovskite. It is very likely that the small change observed around 5500 cm^{-1} (Fig. 4a) can be associated with the 5 % of s-CNTs content in the nominally metallic sample.

The main features in the difference spectra of the composite samples are related to the nanotubes. Carbon nanotubes are sensitive to their environment: contacting with other materials usually results in charge transfer to some extent. The direction and amount of electrons transferred depends on the electronic structure of both materials. Since pristine nanotubes show no photoresponse, the observed changes must originate in the different amount of charge transfer from $MAPbI_3$ in case of measurements under dark/illuminated conditions.

We can consider the composite sample as a semiconductor heterojunction (Fig. 5) similar to what was suggested by Schulz et al.[21]. By forming the contact between the CNTs and $MAPbI_3$

View Article Online
DOI: 10.1039/C7NR06136F

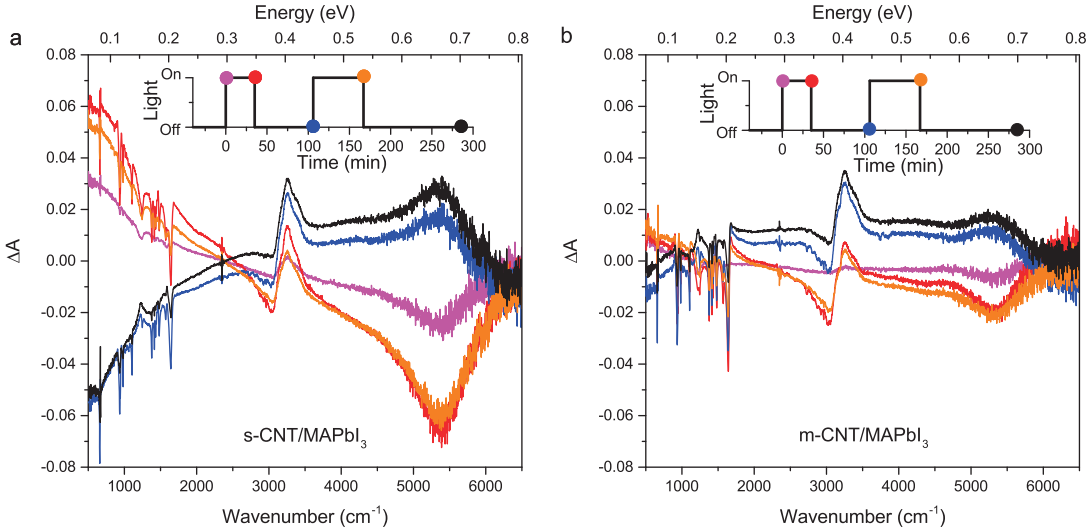

Fig. 3 Difference spectra of the optical absorption between the illuminated and dark samples of a) s-CNT/$MAPbI_3$ composite, where both the free charge carrier part (low wavenumbers) and the S_{11} transition show changes, and b) m-CNT/$MAPbI_3$ composite. In the free-carrier absorption region (<2000 cm^{-1}), the spectrum is unaffected by illumination. For the measurement sequence see color code in the inset.

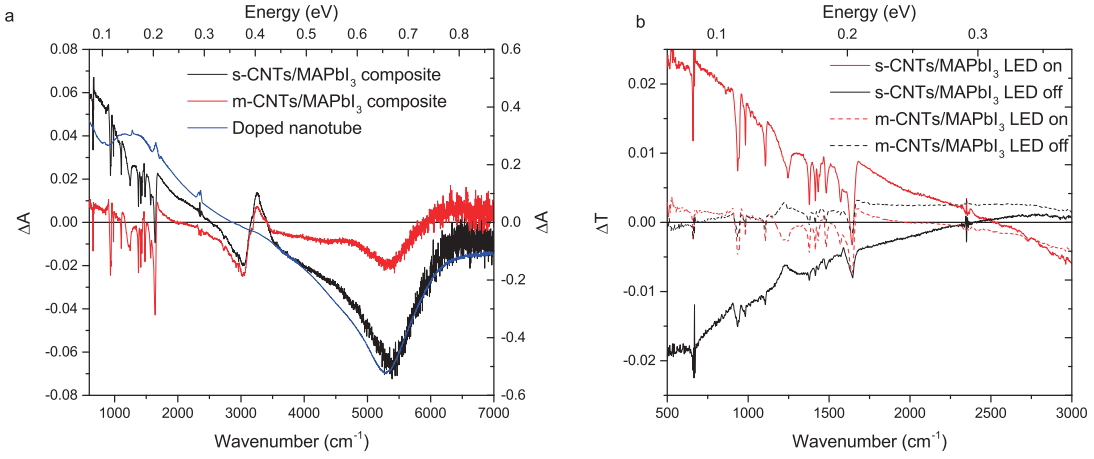

Fig. 4 a) Comparison of the light-induced changes of semiconducting and metallic nanotube composite samples with chemically doped CNTs. b) Comparison of the change in transmission (without normalization) in case of semiconducting and metallic nanotube composite samples. Metallic nanotubes show negligible change compared to the semiconducting tubes upon turning on or off the light.

the bands shift in order to align the Fermi levels. The conduction and valence bands bend to compensate for the different energy levels on the two sides of the junction. The band bending is a result of electron transfer from one side to the other. While $MAPbI_3$ behaves like a bulk semiconductor where the band far from the junction is unaffected, in the nanotube the band shifting is extended throughout the whole length of the tube due to the unscreened Coulomb interaction resulting from the one dimensional nature of the nanotube.[35] Thus, instead of bending, the bands of the nanotube are shifted similar to gating or chemical doping. The main difference between the two types of heterojunctions is that while in the semiconducting case the charge transfer affects the highest occupied Van Hove singularity creating a high density of states at the Fermi level (Fig. 5b), in the metallic case the shift does not change the number of states due to the energy independent density of states of the metallic nanotubes (Fig. 5e). The amount of charge transfer depends on the electronic properties in the same way as the band gap of the materials. The charge transfer between the two materials can be directly observed by electrical transport measurements as well (Supporting Information, Fig. S4). To elucidate the origin of the observed light-induced changes we investigated the time dependence with a series of illuminated and dark measurements.

Figure 6 shows the time dependence of the difference spectrum in the free carrier region for the s-CNT/$MAPbI_3$ composite. It consists of a rapid component in the variation of the optical density and a slow one, which extends to a timescale of tens of minutes in the case of illumination. When the light is switched off, after the initial faster decrease it takes more than an hour to relax back to the original dark state.

The change in optical absorption is coming from the diffusion of the photo-excited electrons through the interface into the carbon nanotubes. Even the small number of photoelectrons (of the order of 10^{15} cm^{-3}) can produce a noticeable change because

View Article Online
DOI: 10.1039/C7NR06136F

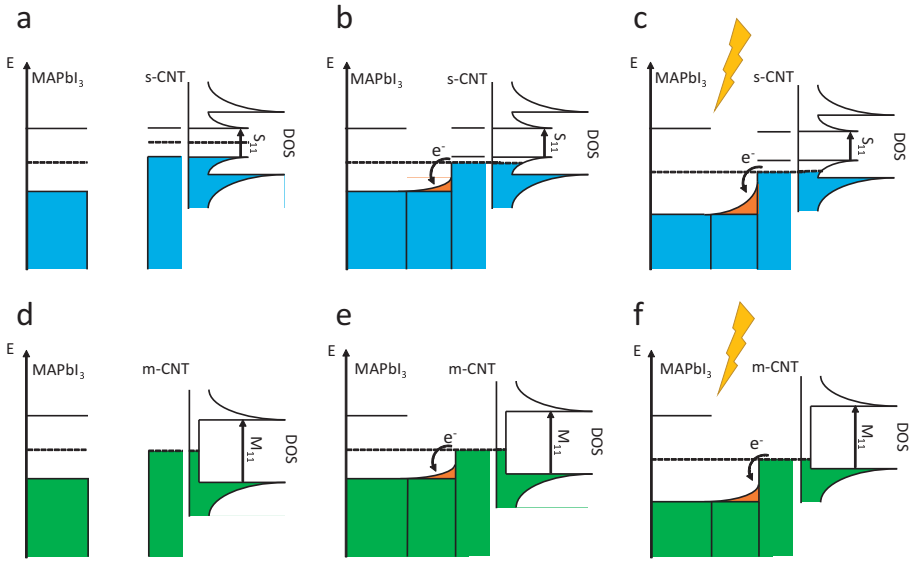

Fig. 5 a) Energy band of $MAPbI_3$ and an s-CNT before forming the contact. b) Band alignment in s-CNTs/$MAPbI_3$ heterojunction in dark (the band of the $MAPbI_3$ bends to compensate for the energy level differences); and c) after illumination. d) Energy band of $MAPbI_3$ and an m-CNT before forming the contact. e) Band alignment in m-CNTs/$MAPbI_3$ heterojunction in dark; and f) after illumination.

they occupy the first excited Van Hove singularity with high density of states. As this process results in a partially filled band, the number of free carriers increases, resulting in low-frequency absorption. At the same time, as there are less available final states for the S_{11} optical excitation within the CNTs, the absorption around 5500 cm^{-1} decreases. The slow change of the optical density has a different origin. Similar, extremely slow variations have been observed in this family of materials[23–25] and ascribed to the decrease of the organic cation binding energy due to illumination. The organic cations in this less bound state can distort the metal halide cage. It is known that the bandgap of the organo-halide perovskites depends on the metal-halide-metal bond angle and distance. The light-induced weakening of the bonds between the organic cation and the metal halide cage in turn changes slightly the bandgap of the material. In this new condition the adjustment of the Fermi levels induces a carrier flow through the interface to establish the new charge balance. This change as reported in Ref. 24 is reversible on a similar timescale as observed here. This simplified picture is also consistent with the response obtained for the m-CNT/$MAPbI_3$ composite. All the changes in the charge flow happen at E_F, at the very low density of states region of the carbon nanotubes that does not produce measurable changes in the optical density. This does not mean that there is no charge flow towards the metallic CNTs; however, this charge flow does not produce enough free carriers to influence the photocurrent significantly. In other words, for efficient free carrier extraction one needs to use s-CNTs, that have been the choice in previous studies.[9,21,22]

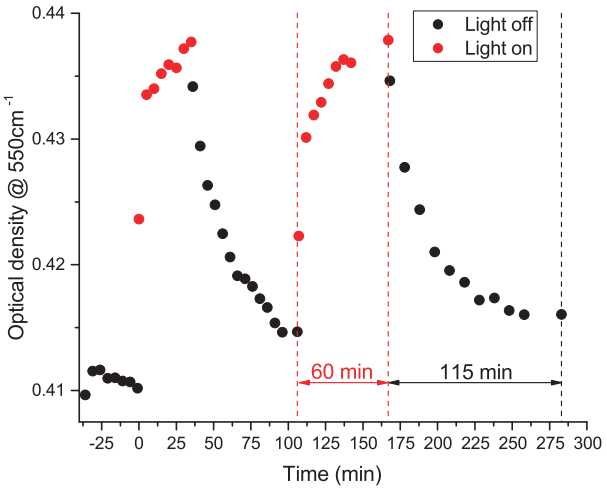

Fig. 6 Time dependence of the light-induced changes in the free-carrier response region (550 cm^{-1}). After an initial fast response, it shows a slow one both in the "on" and "off" state extending to tens of minutes.

4 Conclusions

The simultaneous and opposite change in the S_{11} and Drude peak and the absence of increase in the D band intensity in the Raman spectrum of the CNT/$MAPbI_3$ composites narrows down the ex-

View Article Online
DOI: 10.1039/C7NR06136F

planation of the observed changes to charge transfer between the two materials upon visible light illumination. We found that the time dependence of the nanotube optical features follows that of free standing $MAPbI_3$ films, showing a fast and a slow component. We have identified a fast component, that is very likely to come from the photoexcited carriers in $MAPbI_3$. This response is important in CNT/$MAPbI_3$ composite detectors, sensors, where a fast response is required and the signal is amplified by the peculiar band structure of the CNTs.[15] The charge transfer by the slow component in the optical response, ascribed to the structural, bond-angle relaxation upon illumination, followed by Fermi level alignment is useful in solar cell applications. In this case fast response is not a requirement since the material is exposed to constant illumination in time. Nevertheless, it is likely that for both components, fast and slow, the quality of the interface plays a role, whose optimization should be addressed in the future in order to reduce the trap density.

5 Acknowledgement

Work in Budapest was supported by the Hungarian National Research Fund (OTKA) through grant no. NK 105691 and by the European Structural and Investment Funds jointly financed by the European Commission and the Hungarian Government through grant no. VEKOP-2.3.2-16-2016-00011 and VEKOP-2.3.3-15-2016-00001. Á.P. gratefully acknowledges support from the János Bolyai Fellowship of the Hungarian Academy of Sciences and from the National Research, Development and Innovation Office - NKFIH PD 121320. Special thanks are due to Zoltán Dankházi at SEM Laboratory, Research and Instrument Core Facility (RICF), Faculty of Science, Eötvös University, Budapest. In Lausanne the research was financed by the Swiss National Science Foundation and by the ERC Advanced Grant Picoprop (670918).

Conflict of interest

There are no conflicts to declare.

References

1 H.-S. Kim, C.-R. Lee, J.-H. Im, K.-B. Lee, T. Moehl, A. Marchioro, S.-J. Moon, R. Humphry-Baker, J.-H. Yum, J. E. Moser, M. Grätzel and N.-G. Park, *Sci. Rep.*, 2012, **2**, 591–1–7.

2 G. Xing, N. Mathews, S. Sun, S. S. Lim, Y. M. Lam, M. Grätzel, S. Mhaisalkar and T. C. Sum, *Science*, 2013, **342**, 344–347.

3 M. A. Green, A. Ho-Baillie and H. J. Snaith, *Nat. Photon.*, 2014, **8**, 506–514.

4 X. Mettan, R. Pisoni, P. Matus, A. Pisoni, J. Jaćimović, B. Náfrádi, M. Spina, D. Pavuna, L. Forró and E. Horváth, *J. Phys. Chem. C*, 2015, **119**, 11506–11510.

5 A. Pisoni, J. Jaćimović, O. S. Barišić, M. Spina, R. Gaál, L. Forró and E. Horváth, *J. Phys. Chem. Lett.*, 2014, **5**, 2488–2492.

6 M. Saliba, T. Matsui, J. Y. Seo, K. Domanski, J. P. Correa-Baena, M. K. Nazeeruddin, S. M. Zakeeruddin, W. Tress, A. Abate, A. Hagfeldt and M. Grätzel, *Energy Environ. Sci.*, 2016, **9**, 1989–1997.

7 Research Cell Efficiency Records; http://www.Nrel.Gov/Ncpv/Images/Efficiency_Chart.jpg (accessed: February 2016).

8 U. Bach, D. Lupo, P. Comte, J. E. Moser, F. Weissortel, J. Salbeck, H. Spreitzer and M. Grätzel, *Nature*, 1998, **395**, 583–585.

9 S. N. Habisreutinger, T. Leijtens, G. E. Eperon, S. D. Stranks, R. J. Nicholas and H. J. Snaith, *J. Phys. Chem. Lett.*, 2014, **5**, 4207–4212.

10 S. N. Habisreutinger, T. Leijtens, G. E. Eperon, S. D. Stranks, R. J. Nicholas and H. J. Snaith, *Nano Lett.*, 2014, **14**, 5561–5568.

11 K. Aitola, K. Sveinbjornsson, J. P. Correa-Baena, A. Kaskela, A. Abate, Y. Tian, E. M. J. Johansson, M. Grätzel, A. Hagfeldt and G. Boschloo, *Energy Environ. Sci.*, 2016, **9**, 461–466.

12 Z. Li, S. A. Kulkarni, P. P. Boix, E. Shi, A. Cao, K. Fu, S. K. Batabyal, J. Zhang, Q.Xiong, L. H. Wong, N. Mathews and S. G. Mhaisalkar, *ACS Nano*, 2014, **7**, 6797–6804.

13 F. J. Wang, M. Endo, S. Mouri, Y. Miyauchi, Y. Ohno, A. Wakamiya, Y. Murata and K. Matsuda, *Nanoscale*, 2016, **8**, 11882–11888.

14 M. Spina, M. Lehmann, B. Náfrádi, L. Bernard, E. Bonvin, R. Gaál, A. Magrez, L. Forró and E. Horváth, *Small*, 2015, **11**, 4824–4828.

15 M. Spina, B. Náfrádi, H. M. Tóháti, K. Kamarás, R. Gaál, L. Forró and E. Horváth, *Nanoscale*, 2016, **8**, 4888–4893.

16 L. J. Yang, S. Wang, Q. S. Zeng, Z. Y. Zhang and L. M. Peng, *Small*, 2013, **9**, 1225–1236.

17 J. Y. Jeng, Y. F. Chiang, M. H. Lee, S. R. Peng, T. F. Guo, P. Chen and T. C. Wen, *Adv. Mater.*, 2013, **25**, 3727–3732.

18 Y. H. Shao, Z. G. Xiao, C. Bi, Y. B. Yuan and J. S. Huang, *Nat. Commun.*, 2014, **5**, 5784–1–7.

19 T. Chen, L. B. Qiu, Z. B. Cai, F. Gong, Z. B. Yang, Z. S. Wang and H. S. Peng, *Nano Lett.*, 2012, **12**, 2568–2572.

20 X. Y. Xia, S. S. Wang, Y. Jia, Z. Q. Bian, D. H. Wu, , L. H. Zhang, A. Y. Cao and C. H. Huang, *J. Mater. Chem.*, 2010, **20**, 8478–8482.

21 P. Schulz, A.-M. Dowgiallo, M. Yang, K. Zhu, J. L. Blackburn and J. J. Berry, *J. Phys. Chem. Lett.*, 2016, **7**, 418–425.

22 R. Ihly, A.-M. Dowgiallo, M. Yang, P. Schulz, N. J. Stanton, O. G. Reid, A. J. Ferguson, K. Zhu, , J. J. Berry and J. L. Blackburn, *Energy Environ. Sci.*, 2016, **9**, 1439–1449.

23 R. Gottesman, E. Haltzi, L. Gouda, S. Tirosh, Y. Bouhadana, A. Zaban, E. Mosconi and F. De Angelis, *J. Phys. Chem. Lett.*, 2014, **5**, 2662–2669.

24 R. Gottesman, L. Gouda, B. S. Kalanoor, E. Haltzi, S. Tirosh, E. Rosh-Hodesh, Y. Tischler, A. Zaban, C. Quarti, E. Mosconi and F. De Angelis, *J. Phys. Chem. Lett.*, 2015, **6**, 2332–2338.

25 R. Gottesman and A. Zaban, *Acc. Chem. Res.*, 2016, **49**, 320–329.

26 A. A. Green and M. C. Hersam, *Nano Lett.*, 2008, **8**, 1417.

27 Z. C. Wu, Z. H. Chen, X. Du, J. M. Logan, J. Sippel, M. Nikolou, K. Kamaras, J. R. Reynolds, D. B. Tanner, A. F. Hebard and A. G. Rinzler, *Science*, 2004, **305**, 1273–1276.

28 A. Poglitsch and D. Weber, *J. Chem. Phys.*, 1987, **87**, 6373–6378.

View Article Online
DOI: 10.1039/C7NR06136F

29 E. Horváth, M. Spina, Z. Szekrényes, K. Kamarás, R. Gaal, D. Gachet and L. Forró, *Nano Lett.*, 2014, **14**, 6761–6766.
30 I. Ka, L. F. Gerlein, R. Nechache and S. G. Cloutier, *Sci. Rep.*, 2017, **7**, 45543.
31 T. Baikie, Y. Fang, J. M. Kadro, M. Schreyer, F. Wei, , S. G. Mhaisalkar, M. Grätzel and T. J. White, *J. Mater. Chem. A*, 2013, **1**, 5628–5641.
32 N. Onoda-Yamamuro, T. Matsuo and H. Suga, *J. Phys. Chem. Solids*, 1990, **51**, 1383–1395.
33 Á. Pekker and K. Kamarás, *Phys. Rev. B*, 2011, **84**, 075475.
34 F. Borondics, K. Kamarás, M. Nikolou, D. B. Tanner, Z. Chen and A. G. Rinzler, *Phys. Rev. B*, 2006, **74**, 045431.
35 F. Léonard and J. Tersoff, *Phys. Rev. Lett.*, 1999, **83**, 5174–5177.